European Journal of Pharmaceutics and Biopharmaceutics 142 (2019) 204–215

Contents lists available at ScienceDirect

European Journal of Pharmaceutics and Biopharmaceutics

journal homepage: www.elsevier.com/locate/ejpb

Research paper

Pitfalls in analyzing release from chitosan/tripolyphosphate micro- and nanoparticles

Yuhang Cai[1], Yakov Lapitsky*

Department of Chemical Engineering, University of Toledo, Toledo, OH 43606, United States

ARTICLE INFO

Keywords:
Chitosan
Polyelectrolyte
Nanoparticles
Drug release
Sample and separate method

ABSTRACT

Submicron particles prepared by complexing chitosan with tripolyphosphate (TPP) attract widespread interest as potential drug, gene and vaccine delivery vehicles, and many published studies examine their release properties. Despite these sustained efforts, however, literature on the release performance of chitosan/TPP micro- and nanoparticles is filled with conflicting results, with some reporting nearly instantaneous release, while others showing the release to be sustained for up to multiple days. To resolve these opposing findings, we recently postulated that the *in vitro* release profiles obtained from chitosan/TPP particles by the standard "sample and separate" or "solvent replacement" method (where the solvent was periodically replaced with fresh buffer and analyzed for the released bioactive molecule content) may have been subject to strong experimental artifacts and not have reflected their true release behavior. To explore this possibility, here we examine several experimental artifacts that may arise during such *in vitro* experiments and show that conflicting findings on release from chitosan/TPP particles can arise from: (1) incomplete particle separation from the release media upon centrifugation; (2) irreversible particle coagulation; and (3) failure to maintain sink conditions. Moreover, we show that some of the longer-lasting release profiles may reflect the use of physiologically irrelevant (low-ionic-strength) release media. By analyzing and discussing these effects, this article provides guidelines for obtaining more reliable release profiles for chitosan/TPP micro- and nanoparticles and other/related colloidal carriers.

1. Introduction

In the past two decades, micro- and nanoparticles prepared through the ionotropic gelation of chitosan with tripolyphosphate (TPP) have been extensively investigated for the delivery of drugs, vaccines, and genes [1–4]. This broad interest stems from their several attractive properties, such as forming under very mild conditions (i.e., by simply mixing TPP into dilute chitosan solutions), preserving the bioactivity of their sensitive payloads [5,6], being mucoadhesive [7], and enhancing molecular penetration across epithelial layers [8,9]. Despite the many academic studies performed on these materials, however, the reported *in vitro* release profiles obtained with chitosan/TPP particles vary significantly, even when the same model payload and similar release media (e.g., phosphate buffer) are used. Some studies, for instance, indicate immediate payload release [10–12], while others show release that is sustained over timescales as long as weeks [6,13–15]. These opposing findings cloud the understanding of the release properties of chitosan/TPP particles and make their safe and efficacious application difficult to achieve.

The overwhelming majority of *in vitro* release studies on chitosan/TPP particles use two experimental methods. The first is the "sample and separate" (or "solvent replacement") method, where the release media is periodically replaced and tested for its released payload content [10–12,16], while the second is the dialysis method, where particles are placed in a dialysis bag and dialyzed against a release medium, which is maintained at sink conditions (i.e., conditions where payload accumulation in the release media does not appreciably impede its further release) [17–19]. Previous reports have shown that reliable release profiles via the dialysis method can only be achieved when release from the micro- and nanoparticles is much slower than the time required for the released molecules to be eluted from the dialysis bag [20–23]. These studies revealed that, for colloidal carriers that can reversibly bind their payloads (like the chitosan/TPP particles), the measured release from the dialysis bag is slower when particles are used than for the particle-free control, even when the actual release from the particles is immediate [20–22]. This result reflects equilibrium partitioning between the particles and release media – i.e., if a fraction of the releasing solute in the dialysis bag is always bound to the particles, the

* Corresponding author.
E-mail address: yakov.lapitsky@utoledo.edu (Y. Lapitsky).
[1] Current address: Latitude Pharmaceuticals Inc., San Diego, CA 92131, United States.

https://doi.org/10.1016/j.ejpb.2019.06.020
Received 22 March 2019; Received in revised form 17 June 2019; Accepted 17 June 2019
Available online 19 June 2019
0939-6411/

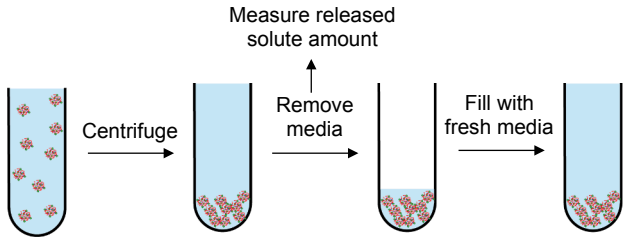

Fig. 1. Schematic representation of the sample and separate method for measuring release kinetics from colloidal particles.

release from the bag is slower, even if the solute transport in and out of the particles is instantaneous. Moreover, these analyses showed that release times obtained under conditions where solute release from the particles is faster than its release from dialysis bags depend strongly on the area-to-volume ratios (and pore structures) of the dialysis bags used; which, when taken together, calls into question much of the chitosan/TPP micro- and nanoparticle release data collected using this method [20,23].

Besides these problems with the dialysis method, conflicting release profiles from chitosan/TPP particles are also seen in studies that use the centrifugation-assisted "sample and separate" or "solvent replacement" method, which has been used in studies on chitosan/TPP particles even more frequently than the aforementioned dialysis method [10–12,16]. The widespread use of this method reflects the wide availability of centrifuges in academic labs and the ability to achieve selective separation of colloidal dispersions by tuning the centrifugation force and time. A drug-loaded chitosan/TPP micro- and nanoparticle dispersion, for instance, is a mixture of soluble drug, chitosan and drug/chitosan complexes, and drug-loaded chitosan/TPP particles [24]. Because the particles are denser than water (and are comparatively large), centrifugation enables one to sediment the chitosan/TPP particles while keeping the other (soluble) components in the supernatant. Since most release profiles obtained from chitosan/TPP particles by the sample and separate method were obtained by separating the particles from the supernatant by centrifugation (see Fig. 1), we hypothesized that inconsistencies in the reported release profiles may have stemmed from four possible artifacts that can occur when the centrifugation-assisted sample and separate method is used. These are described in the paragraphs below.

The first artifact that could strongly distort the release profiles in these experiments is the incomplete recovery of payload-bearing particles upon centrifugation [25,26]. In other words, a weak centrifugal force and short centrifugation time might not remove all the particles from the release media. Such persistence of payload-containing particles in the release media may lead to an overestimation of the release rate, as concentration measurement techniques do not always distinguish between the released molecules and the molecules within the particles (see Supplementary Data, Section A). Conversely, if the particle-loaded molecules in the supernatant are not detected, this incomplete particle recovery may lead to an underestimation of the total amount of release from the chitosan/TPP particles (since the true amount that can be released becomes smaller than that assumed to be present). To prevent this, a high centrifugal force and long centrifugation time may be needed.

The second major issue that could affect the apparent release rates is the extensive centrifugation that is required to fully sequester the particles. Based on this strong centrifugation, our second conjecture is that some of the inconsistency in the reported release profiles could reflect the centrifugation-induced coagulation of chitosan/TPP micro- and nanoparticles into macroscopic gels. Such coagulation is typically irreversible, and therefore (by increasing the diffusion distance) likely extends the release times. This could render the release profiles sensitive to variations in centrifugation methods (i.e., variations in centrifugal force and time). More extensive centrifugation, for instance, could increase the extent of such coagulation and may thus reduce the release rates.

To prevent this coagulation, glycerol beds are sometimes used [11,27,28]. By adding a small amount of glycerol to the bottom of the centrifuge tube, the sedimented particles can be suspended inside the glycerol layer, which limits their irreversible coagulation upon centrifugation. This effect is caused by the dense glycerol (through its interdiffusion with the aqueous buffer) generating a density gradient at the bottom of the tube. Due to this diffusion, and the density of pure glycerol exceeding that of chitosan/TPP particles, the particles remain suspended/dispersed near the bottom of the centrifuge tube rather being deposited and coagulated on its bottom surface. Even when glycerol beds are used, however, it is unclear that the particles remain stable to coagulation over multiple centrifugation/solvent replacement cycles, which could again affect the measured release profiles.

The third possible reason for the opposing literature release rates is the variability in the release media compositions. Because solvent pH and ionic strength can affect both the particle structure [29–31] and payload molecule/particle interactions [24,32,33], this variability in release media compositions undoubtedly results in disparate release characteristics. Many reports, for instance, use phosphate buffered saline (PBS) as the release media [10,11,14]. In these studies, release profiles obtained via the sample and separate method often reveal rapid release before the first solvent replacement step, followed by a plateau (which suggests that all "releasable" payload is rapidly eluted from the particles [10,11,14]). Conversely, the two seminal papers on chitosan/TPP micro- and nanoparticles by Calvo et al. showed that the chitosan/TPP particles can release the protein bovine serum albumin (BSA) for more than one week [34,35]. In their work, however, a salt-free trehalose solution instead of a physiological ionic strength buffer (e.g., PBS) was used as the release medium. It is well-known that salt can diminish the electrostatic binding between oppositely charged proteins and polyelectrolytes [36–38]. Thus, we postulated that this long-term release could result from the choice of salt-free trehalose solution as the release media, where (unlike in a saline environment) BSA could remain associated with the particles due to a strong protein/particle binding.

Further, the fourth possible artifact that could underlie the conflicting reports is that it is commonly ignored that the sampling/solvent replacement frequency (i.e., the time interval between each sampling/solvent replacement step) could affect the release profile, especially when the actual release is fast [20]. This may result from the equilibrium partitioning of the releasing molecules between the liquid media and solid particles where, once equilibrium partitioning is achieved, no further release may occur until the next solvent replacement step. In other words, "sink conditions," which are typically assumed in release experiments, are not maintained and bioactive payload accumulation in the release media impedes its further release. When the release is faster than the sampling frequency (such that equilibrium partitioning between the particles and media is reached before the solvent is replaced), the release profile could be predominantly controlled by the solvent replacement frequency [20]. Thus, we surmised that low solvent replacement frequencies – which are used in many studies showing chitosan/TPP particles to provide release over multi-day timescales [6,14,15,34,35] – may lead to much slower apparent release than high solvent replacement frequencies and introduce significant experimental artifacts into the release rate measurements.

In summary, we hypothesized that many of the conflicting release profiles obtained by analyzing chitosan/TPP micro- and nanoparticles via the "sample and separate" (or solvent replacement) method were caused by: (1) irreversible micro- and nanoparticle coagulation during centrifugation; (2) failure to completely separate the particles from the supernatant; (3) inconsistency in the release media compositions used; and (4) use of varied (and inappropriately selected) solvent replacement frequencies. To explore these hypotheses, we investigated the

above artifacts using BSA as the model biomolecular payload. Because the effects investigated in this study on submicron chitosan/TPP particles also likely apply to other micro- and nanoscale delivery systems, such as those prepared from other polyelectrolytes or (as shown in prior reports [25,26,39–41]) even other polymers, emulsions or lipids, findings from this analysis may also be instructive for characterizing release from other colloidal materials.

2. Materials and methods

2.1. Materials

Chitosan (viscosity average molecular weight = 154 kDa as determined by capillary viscometry [42]), TPP, BSA, fluorescein isothiocyanate (FITC) and dimethyl sulfoxide (DMSO) were all purchased from Sigma-Aldrich (St. Louis, USA). Micro BCA protein assay, hydrochloric acid (HCl), sodium chloride (NaCl) and sodium hydroxide (NaOH) were purchased from Fisher Scientific (Fair Lawn, NJ). The chitosan degree of deacetylation (DD) was estimated to be 86% via pH titration [43]. All materials were used as received and Millipore Direct-Q 3 deionized water (DI water) with a resistivity of 18.2 MΩ·cm was used in all experiments.

2.2. Preparation of FITC-labeled chitosan

To facilitate measurement of particle recovery during centrifugation, the chitosan was labeled with FITC as described previously [24]. Briefly, 5.7 mL of FITC solution in DMSO (1 mg/mL) were added to 150 mL of aqueous 0.2 wt% chitosan solution (adjusted to pH 4.0 with HCl) and allowed to react in the dark at room temperature for 3 h. The resulting FITC-labeled chitosan (FITC-chitosan) was then dialyzed against DI water for 24 h (using a Spectra/Por regenerated cellulose membrane, MWCO = 2000) three times. Analyzing the unreacted FITC concentration in the dialysate revealed that approximately 0.3% of the chitosan amine groups were labeled with FITC. The purified FITC-chitosan solution was then lyophilized and stored (at −18 °C) until use.

2.3. Preparation of BSA-loaded chitosan/TPP particles

To prepare 0.1 wt% chitosan solutions, 0.08 g chitosan was placed in 80 mL of deionized water and, after adding 63 μL of 6 M HCl, stirred with a 12 mm × 4 mm magnetic stir bar at 150 rpm overnight. Aqueous 0.2 wt% BSA and 0.125 wt% TPP solutions were then prepared, and all solutions were adjusted to pH 5.5 using either 1 M NaOH or 0.2 M HCl. To prepare the BSA-loaded chitosan/TPP particle dispersions, 4 mL of 0.2 wt% BSA solution was added to 10 mL of 0.1 wt% chitosan solution at a rate of 2 drops/s and stirred at 800 rpm for 30 min. Two mL of 0.125 wt% TPP solution was then added dropwise into the chitosan/BSA mixture at the same rate, whereupon the chitosan/BSA/TPP mixture was stirred overnight. Similarly, BSA-loaded FITC-chitosan/TPP particles were prepared by the same method, except using the FITC-labeled chitosan instead of commercial chitosan. Further, to explore the effect of BSA loading on the particle recovery during centrifugation, BSA-free FITC-chitosan/TPP particles were prepared. To keep the chitosan and TPP concentrations consistent with those in the BSA-loaded chitosan/TPP particle dispersions, 4 mL of pH-matched water was added during the particle preparation instead of the BSA solution.

2.4. Particle recovery via centrifugation

BSA and chitosan recovery via centrifugation were studied together to explore the centrifugal force and centrifugation time effects on particle recovery. To probe the centrifugation condition effect on the chitosan recovery, BSA-free and BSA-loaded FITC-chitosan/TPP particle dispersions were centrifuged at 10 °C with centrifugal forces ranging between 2.1×10^4 and $3.0 \times 10^5 g$ (with the centrifugation time fixed at 30 min) and centrifugation times ranging between 15 min and 2 h (with the centrifugal force fixed at $3.0 \times 10^5 g$) using a Beckman ultracentrifuge (Ann Arbor, MI; motor model: SW 55Ti). As control experiments, TPP-free FITC-chitosan solutions and FITC-chitosan/BSA mixtures with chitosan/BSA concentrations matching those of the BSA-loaded chitosan/TPP particle dispersions were centrifuged under identical centrifugation conditions. The percent chitosan recovery was calculated as follows:

$$\%\ Chitosan\ Recovery = \left(1 - \frac{C_f}{C_i}\right) \times 100\% \quad (1)$$

where C_f was the final chitosan concentration after centrifugation and C_i was the initial chitosan concentration before centrifugation.

Similar to the chitosan recovery measurements, BSA recovery measurements were performed at varying centrifugation conditions using BSA-loaded chitosan/TPP particle dispersions, chitosan/BSA mixtures and molecular BSA solutions with matching chitosan/BSA concentrations. The supernatant BSA concentrations were determined using the Micro BCA protein assay, where the presence of chitosan/TPP particles did not significantly affect the determination of the total supernatant BSA concentration (see Supplementary Data, Section A). The BSA recovery was then calculated using an expression analogous to Eq. (1).

2.5. BSA release from gel pellets

To examine the release kinetics from the gel pellets that formed from chitosan/TPP micro- and nanoparticles upon centrifugation, 5 mL aliquots of BSA-loaded chitosan/TPP particle dispersions were placed in the ultracentrifuge tubes. After centrifuging these dispersions for 30 to 90 min at 2.1×10^4 to $3.0 \times 10^5 g$ and 10 °C (which coagulated the particles into pellets), 80% of the supernatant from each sample was collected and replaced with 1.25× PBS buffer, so that the final dispersions contained 1× PBS (pH 7.4). The centrifuge tubes were then placed into an Eppendorf Thermomixer set to 37 °C and a 220 rpm agitation speed. After a specific time interval (which ranged between 5 min and 24 h), 80% of the supernatant was replaced with fresh 1× PBS (pH 7.4). Since the gel pellets adhered to the bottoms of centrifuge tubes, only the tops of the pellets were exposed to the release media (which meant that release only occurred through the tops of the pellets). The amount of BSA released during each interval between solvent replacement steps was calculated as:

$$m_i = V\left[C_{A,i} - C_{A,i-1}(1 - R)\right] \quad (2)$$

where m_i was the mass of the BSA released between the $(i-1)$th and ith sampling/solvent replacement steps, and $C_{A,i}$ and $C_{A,i-1}$ were the supernatant BSA concentrations after the ith and $(i-1)$th solvent replacements. When $i = 1$, $C_{A,0}$ equaled to the initial supernatant BSA concentration (i.e., before the dispersion was mixed with the PBS). R was the solvent replacement ratio, which was the supernatant volume fraction replaced during each solvent replacement step (and was 0.8 for all experiments in this study). Finally, V was the total release media volume (5 mL). Based on this, the percent release (which quantified the loaded BSA fraction released) and normalized percent release (which was normalized to the plateau percent release at the end of the release experiment) was determined as:

$$\%\ Released = \frac{\sum m_i}{m_0} \times 100\% = \frac{\sum V\left[C_{A,i} - C_{A,i-1}(1-R)\right]}{m^{\mathrm{Tot}}_{\varepsilon}} \times 100\% \quad (3)$$

$$Normalized\ \%\ Released = \frac{\sum m_i}{m_\infty} \times 100\% = \frac{\sum V\left[C_{A,i} - C_{A,i-1}(1-R)\right]}{m_\infty} \times 100\% \quad (4)$$

where $\sum m_i$ was the cumulative mass of BSA released, m_0 was the initial amount of BSA within the gel pellet, m_∞ was the amount of BSA released at the end of the experiment (which was taken to be the amount of releasable BSA), m^{Tot} was the total BSA mass added to the chitosan/

TPP dispersion during particle formation, and ε was the payload recovery efficiency (i.e., the fraction of BSA recovered from the supernatant through centrifugation during the pellet formation steps), which was measured as described in Section 2.4 and varied with the centrifugation conditions.

2.6. BSA release from dispersed particles

To prevent BSA-loaded particle coagulation into pellets, a glycerol bed was used. Here, 120 μL of glycerol was carefully added (dropwise) to each particle dispersion. Because glycerol was more dense than water (glycerol density = 1.26 g/cm^3), it quickly sedimented to the bottoms of the centrifuge tubes and, through diffusion, generated density gradients there. Due to these gradients, the density of pure glycerol exceeding that of chitosan/TPP particles (see Supplementary Data, Section B) and, possibly, the high glycerol viscosity (906 cP [44]; which likely hindered interparticle and particle-tube collisions), particle deposition and coagulation on the bottoms of the centrifuge tubes was inhibited. Furthermore, glycerol is a water-soluble, nonionic small molecule, which does not appear to strongly interact with chitosan/TPP particles. Thus, the glycerol-protected particles can be easily redispersed by vortexing the sediment. This redispersion is readily demonstrated by dynamic light scattering (DLS), which shows that the 40–1000 nm particle size does not change much after this centrifugation and redispersion process (see Supplementary Data, Section C). Therefore, to study the release properties of dispersed particles in our experiment, glycerol beds were added to the bottoms of centrifuge tubes to help redisperse the particles after each centrifugation and solvent replacement step.

To explore how the ionic strength of the release media alters the measured release rates from the colloidal dispersions, we performed a BSA release experiment using 5 wt% trehalose solutions (to mimic the release conditions used in the seminal work by Calvo et al. [34,35]) as the release media. To compare the salt-free conditions used by Calvo et al. with typical physiological ionic strengths, two ionic strength levels (0 and 150 mM NaCl) were used. Here, 2.5 g batches of chitosan/TPP particle dispersions (prepared from 0.1 wt% chitosan solutions) were mixed with 2.5 g aliquots of 10 wt% trehalose and either 0 or 300 mM NaCl (pH 6.0) solution inside of centrifuge tubes (thus generating release media that contained 5 wt% trehalose and either 0 or 150 mM NaCl).

Prior to each centrifugation/solvent replacement step, the glycerol beds (120 μL each) were added as described previously. After each dispersion was centrifuged at $3.0 \times 10^5 g$ and 37 °C for 1 h, 4 g of the supernatant in each tube was replaced with a fresh mixture of 5 wt% trehalose (pH 6.0) and either 0 or 150 mM NaCl ($R = 0.8$). The dispersions were then vortex-mixed for 20 s, and another 120 μL of glycerol was immediately added to each dispersion, whereupon the particles were immediately centrifuged again (as each centrifugation step already provided 1 h of release time). This procedure was then repeated several more times until the release profile reached a plateau.

To also probe the sampling/solvent replacement frequency effect on the measured release profile, a similar procedure was used (with salt-free trehalose solution used as the release media). The time interval between sampling steps, however, was varied from 1 to 12 h. Here, the 1 h centrifugation time was again counted as part of each time interval, as the release persisted during the 1 h centrifugation step and the ultracentrifuge was thermostated at 37 °C (i.e., the same temperature as that used for the rest of the release experiment). To achieve this constant release temperature when the time interval exceeded 1 h, the dispersions were incubated in an Eppendorf Thermomixer at 37 °C (operated at a 220-rpm agitation speed) until the final hour of the time interval, during which the dispersions were centrifuged. To provide a 12 h time interval, for instance, the dispersions were placed in the Thermomixer for 11 h and then centrifuged for 1 h. The release profiles were then calculated as described in Section 2.5.

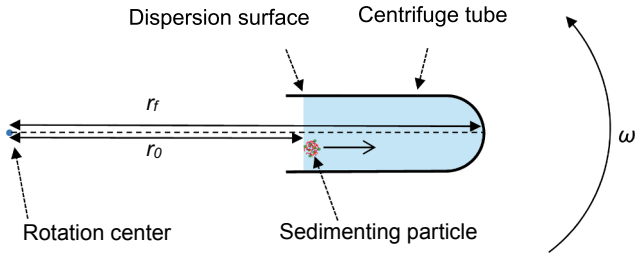

Fig. 2. Schematic representation of particle sedimentation in a centrifuge tube inside a swinging bucket centrifuge rotor.

3. Results and discussion

3.1. Centrifugation procedure effects on particle recovery

A rough (and optimistic) estimate of the centrifugation time and speed needed to separate all the particles from the supernatant can be obtained using Eq. (5) [45]:

$$t = \frac{9\eta \ln(r_f/r_0)}{2\Delta\rho a^2\omega^2} \quad (5)$$

where Δρ is the density difference between the particles and solvent, a is the nanoparticle radius, η is the solvent viscosity, ω is the centrifugation speed (rad/s), r_0 is the radial position of the dispersion surface and r_f is the radial position at the bottom of the centrifuge tube (see Fig. 2). This equation is derived from Stokes' law (which applies because the Reynolds number for colloidal chitosan/TPP particle sedimentation is on the order of 10^{-2} [46]). Additionally, this equation assumes that the particles are spherical and sediment at their terminal velocity, and that the centrifuge tubes rotate in parallel to the ground. This equation, however, ignores: (1) the diffusion term, by assuming that the particle diffusion is much slower than its sedimentation; and (2) the hydrodynamic interactions between the particles. Thus, since both of these effects hinder sedimentation [47–49], Eq. (5) provides a low (i.e., optimistic) estimate of the centrifugation time.

When $a = 50$ nm, $\Delta\rho \approx 0.07$ g/mL (based on chitosan/TPP gel pellet and PBS densities being 1.08 and 1.01 g/mL, respectively), $\eta = 1.3$ cP (viscosity of water at 10 °C [50]), $r_0 = 6.1$ cm, $r_f = 10.9$ cm and $\omega = 2094$ rad/s (20,000 rpm), as is roughly the case in the present study, the time required for the particles from the surface of the dispersion to sediment to the bottom of the centrifuge tube is approximated by Eq. (5) at roughly 70 min. The above conditions correspond to a centrifugal force of $2.7 \times 10^4 g$, which is close to those typically reported in the literature. The centrifugation time estimated above, however, is considerably longer than that typically used (30 min) [14,35,51–55]. Further, the sedimentation efficiency is affected by both diffusion and interparticle hydrodynamic interactions. If the sedimentation speed is not high enough, for instance, diffusion could substantially increase the time required to sediment the particles [47–49]. Similarly, hydrodynamic interactions can significantly hinder sedimentation once the dispersions become concentrated near the bottoms of the tubes [49]. Based on Eq. (5) and these effects, full separation of particles from the supernatant likely requires long centrifugation at high speeds.

To experimentally confirm the above analysis, recovery of chitosan/TPP micro- and nanoparticles (both empty and BSA-loaded) through ultracentrifugation was measured at various ultracentrifugation speeds and times. When the centrifugation time was fixed at 30 min (which is typical), chitosan recovery from the chitosan/TPP particles increased from 60 to 85% as the centrifugal force was increased from 2.1×10^4 to $3.0 \times 10^5 g$ (see Fig. 3a). Thus, at this frequently-used short centrifugation time, a significant portion of the chitosan/TPP particles was

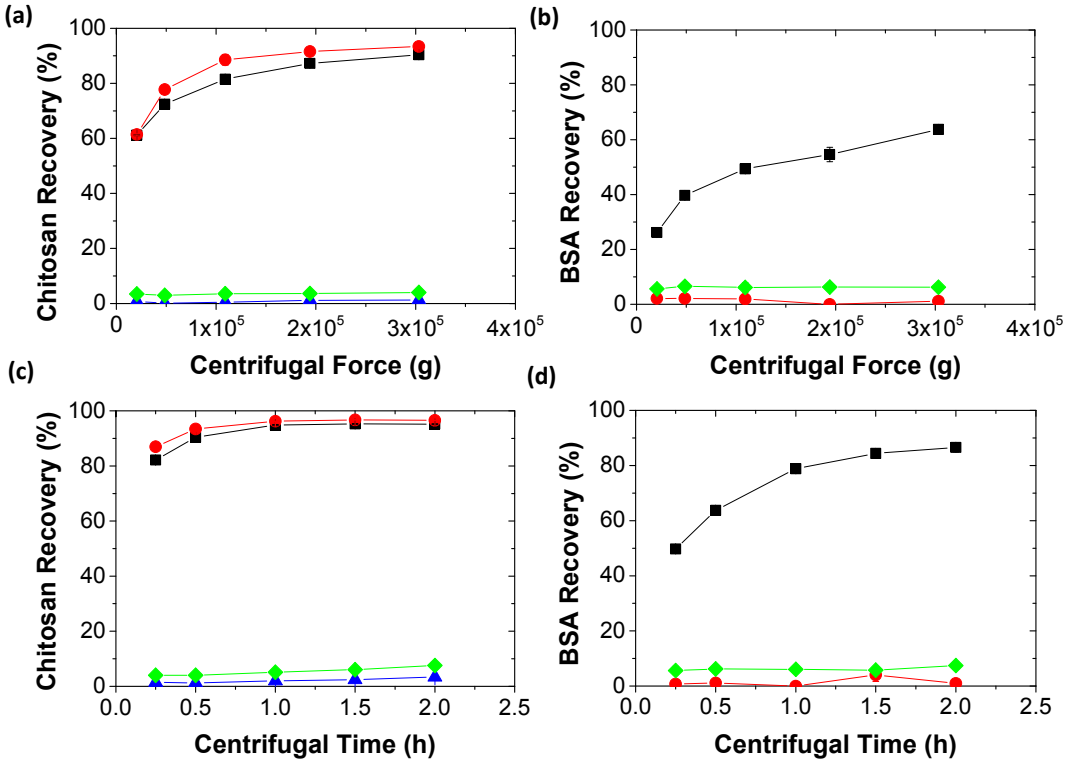

Fig. 3. The effects of (a, b) centrifugal force and (c, d) centrifugation time on the (a, c) chitosan recovery from (■) chitosan/TPP particles, (●) BSA-loaded chitosan/TPP particles, (▲) TPP-free chitosan and (◆) TPP-free chitosan/BSA mixtures; and (b, d) BSA recovery from (■) BSA-loaded chitosan/TPP particles, (●) chitosan- and TPP-free BSA solutions and (◆) TPP-free chitosan/BSA mixtures. The centrifugation force effects were investigated using a 30 min centrifugation time, while the centrifugation time effects were probed at a constant centrifugal force of $3.0 \times 10^5 g$. The error bars (which are largely obscured by the symbols) are standard deviations, while the lines are guides to the eye.

not separated from the supernatant at the typical, 2–4 × $10^4 g$ centrifugal forces used in release experiments on chitosan/TPP particles [14,35,51–55].

When BSA was loaded into chitosan/TPP particles, the chitosan recovery increased (Fig. 3a), likely because: (1) particles became larger upon BSA uptake (see Supplementary Data of Ref. [24]); and (2) since the pH used exceeded the protein's pI ≈ 4.7–4.9 [56], the negatively charged BSA caused more of the dissolved chitosan to self-assemble into particles [24]. This increase, however, did not greatly diminish the centrifugal force requirement for sedimenting the particles. As a comparison, chitosan recoveries in the control TPP-free chitosan and chitosan/BSA mixtures were all below 5% (Fig. 3a), which confirmed that the vast majority of the chitosan recovery reflected particulate/TPP-crosslinked (rather than soluble) chitosan.

The importance of centrifugal force was further supported by BSA recovery measurements (Fig. 3b). Only 26% of BSA were recovered with the chitosan/TPP particles at the centrifugal force of 2.1 × $10^4 g$. When the centrifugal force increased to 3.0 × $10^5 g$, however, the recovered BSA increased significantly to 64%. Further, like in the case of chitosan recovery, in the absence of chitosan/TPP particles the sedimented protein fraction remained consistently low (well below 10%), which showed that the enhanced protein recovery reflected the sedimentation of particle-bound protein, and not free protein in solution. This increase in the particulate chitosan and protein recovery with the centrifugation force indicated that a very strong centrifugal force was needed to fully separate chitosan/TPP particles from the supernatant.

Similar to the effect of centrifugal force, the particulate chitosan and BSA recovery was also noticeably enhanced by increasing the centrifugation time (Fig. 3c and d). When the centrifugal force was fixed at 3.0 × $10^5 g$, the chitosan recovery increased from 82 to 95% as the centrifugation time for the BSA-free chitosan/TPP particles was increased from 15 min to 2 h (with loading of BSA further raising the particulate chitosan recovery). Similar to the recovery of chitosan, the recovery of BSA increased with the centrifugation time and reached a plateau at around 1.5 h, where nearly all BSA-loaded particles were apparently sedimented (Fig. 3d). In the absence of TPP, however, less than 7% of both chitosan and BSA were removed, even after 2 h at the highest centrifugation speed (which again confirmed that the increased chitosan and BSA recovery reflected the recovery of particulate rather than dissolved species).

Interestingly, the plateau chitosan recovery was achieved sooner than the plateau BSA recovery, which contradicted previous findings that the BSA recovery should be roughly proportional to the chitosan recovery for chitosan/TPP micro- and nanoparticles [24]. This may have reflected the chitosan/TPP particles prepared with FITC-labeled chitosan in the chitosan recovery experiment being larger (z-average diameter = 330 ± 14 nm, as determined by DLS) than those prepared from commercial chitosan for the BSA recovery experiment (z-average diameter = 279 ± 15 nm). The larger particle size obtained with FITC-labeling might have stemmed from the slightly higher hydrophobicity of FITC-labeled chitosan (which may have promoted chitosan/TPP aggregation into slightly larger colloids) and likely made the particles easier to sediment. This hypothesis was confirmed by repeating some of the BSA recovery measurements with FITC-chitosan, where plateau BSA recovery was achieved after 1 h, just like the chitosan recovery in Fig. 3c (see Supplementary Data, Section D). Additionally, since not every chitosan and BSA molecule was incorporated into the particles during the particle formation/BSA uptake process [24], plateau chitosan and BSA recoveries both expectedly remained below 100% (Fig. 3 and Supplementary Data, Fig. S3).

Based on the above analysis, near-quantitative chitosan/TPP particle recovery requires centrifugation times of at least 1.0–1.5 h at a centrifugal force of 3.0 × $10^5 g$. Most literature procedures, however (despite similar particle sizes), use centrifugation time of 30 min and

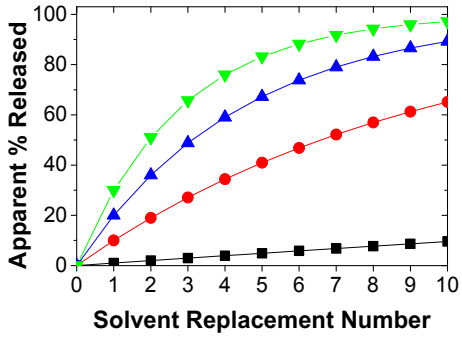

Fig. 4. Model particle recovery effect on the apparent release profile calculated for conditions where (■) 99%, (●) 90%, (▲) 80% and (▼) 70% of the particles were recovered by centrifugation during each solvent replacement step. These model predictions were obtained under the simplifying assumption of no release really occurring (which means that the true release profile should be a flat line overlapping the abscissa).

much-lower centrifugal forces, which typically range between 2×10^4 and $4 \times 10^4 g$ [14,35,51–55]. This weak centrifugation likely fails to separate all the particles from the supernatant, as shown in Fig. 3. The seminal papers on chitosan/TPP by Calvo et al., for example, centrifuged their particles for only 30 min at $4 \times 10^4 g$ [34,35]. This less-extensive centrifugation leads to a lower particle recovery, which not only causes underestimation of their bioactive payload uptake (since this centrifugation is also used during uptake experiments), but also can cause overestimation of release rates. The magnitude of this artifact is demonstrated by the model analysis in Fig. 4, which uses Eq. (3) and, for simplicity, assumes: (1) that all of the bioactive molecule (in this case protein) is initially loaded into particles; (2) that the entire supernatant phase is replaced during each solvent replacement step; (3) that none of the protein is really being released from the particles; and (4) that, as shown in Supplementary Data, Section A, the protein assay does not distinguish between the free protein and particle-loaded protein. When particle recovery in each sampling/solvent replacement step is 99%, roughly 10% of the protein is "released" (i.e., detected in the supernatant due to the persistence of unsedimented particles) after 10 solvent replacement steps. When particle recovery in each solvent replacement step decreases to 70%, however, 97% of the protein is "released" (Fig. 4). Thus, low centrifugal forces and/or short centrifugation times have the potential to produce significant artifacts in the measured release rates by leaving detectable, particle-loaded protein (or other payload) molecules dispersed in the supernatant.

3.2. Coagulation effects and release properties of coagulated particles

Besides recovering nearly all the particles, it is important that the centrifugation procedure does not strongly affect the particle structure and release properties [25]. Yet, particle coagulation into gel-like pellets (see Fig. 5) occurs even at the lowest centrifugal force and shortest centrifugation time analyzed in Fig. 3 (i.e., at a centrifugal force of

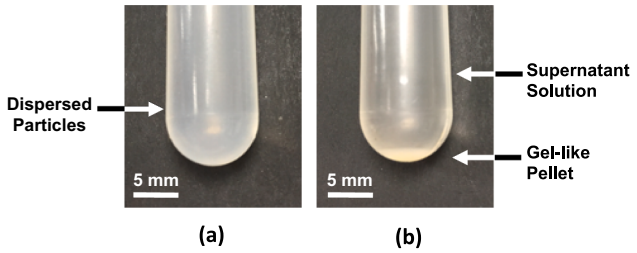

Fig. 5. Photographs of (a) a chitosan/TPP nanoparticle dispersion before centrifugation and (b) the chitosan/TPP gel-like pellet that is obtained after centrifugation due to particle coagulation.

$2.1 \times 10^4 g$ applied over 30 min). This suggests that the high centrifugation intensity needed to fully separate the particles from the supernatant could lead to their irreversible coagulation into macroscopic, gel-like pellets (which could not be fully redispersed even after extensive agitation or ultrasonic treatment).

This particle coagulation could have a drastic impact on measured release rates. For particles with a 500 nm radius and an effective payload diffusivity of 1×10^{-7} cm^2/s (which may be expected for a protein in a water-rich hydrogel network [57]), for instance, the characteristic release time should be on the order of 10 ms [58] (i.e., $\tau \sim R^2/D_A$, where τ is the characteristic release time, R is the particle radius and D_A is the effective payload diffusivity within the particles [46,58]). If the colloidal particles coagulate into a pellet with a radius of 1 mm, however, the release time increases drastically to approximately 1 d. These D_A and τ estimates assume: (1) that the releasing protein molecules exhibit no appreciable binding to the chitosan/TPP particles (since the positive chitosan charges are mostly neutralized in the pH 7.4 PBS release media); and (2) that the particles do not degrade – indeed, if surface or bulk particle degradation does occur during the release process, the release could be even faster. Thus, some of the slower release rates reported in the literature suggest that release may have occurred from macroscale pellets (or at least larger aggregates) rather than dispersed nanoscale particles [6,13,14]. To explore this hypothesis, BSA release from the gel-like pellets obtained upon ultracentrifugation was characterized while varying both centrifugation force and time used to form the gel pellets.

3.2.1. Centrifugal force effect on the release profile

When the centrifugal force increased from 4.8×10^4 to $3.0 \times 10^5 g$, it (as shown in Section 3.1) caused more chitosan and BSA to be collected at the bottoms of the centrifuge tubes (e.g., the BSA recovery increased from roughly 40–64%; Table 1). This accumulation of both BSA and chitosan, however, did not reduce the release rate (Fig. 6a and b), possibly because the gel pellets (which determined the diffusion distance) did not get thicker. Indeed, the pellet thickness, defined as the distance from the bottom of the centrifuge tube to the top of the gel layer, decreased slightly (from 0.16 to 0.13 cm) as the centrifugal force increased (Table 1). Further, the slow BSA release after the initial burst indicated that the gel pellets were stable to dissolution while in pH 7.4 PBS. This stability was likely because the deprotonation of chitosan reduced its aqueous solubility [42], which (even if the TPP was leached) prevented the gel from dissolving (see Supplementary Data, Section E). Another interesting feature of the release data was that, roughly 20–30% of the protein appeared to be retained in the pellet, even when the plateau in the release profile was reached. This retention was highest at the intermediate centrifugal force ($1.1 \times 10^5 g$). Overall, however, the release curves in Fig. 6a and b were all very close, indicating that protein release from the gel pellets was insensitive to the centrifugal force.

3.2.2. Centrifugation time effect on the release profile

Similar to the centrifugal force effect, when the centrifugation time increased from 30 to 90 min, more BSA was collected at the bottoms of

Table 1
Variations in the gel pellet thickness, BSA recovery and apparent BSA diffusivity within the gel with the centrifugal force and centrifugation time (average ± standard deviation).

Centrifugal force (g)	Centrifugation time (min)	Gel thickness (cm)	BSA recovery (%)	$D_A \times 10^7$ (cm^2/s)
4.8×10^4	30	0.16 ± 0.00	39.7 ± 0.3	3.8 ± 0.7
1.1×10^5	30	0.15 ± 0.02	49.4 ± 0.5	3.4 ± 0.5
3.0×10^5	30	0.13 ± 0.00	63.8 ± 1.1	3.8 ± 0.3
3.0×10^5	60	0.10 ± 0.00	78.9 ± 0.2	1.1 ± 0.2
3.0×10^5	90	0.11 ± 0.01	84.4 ± 0.8	1.5 ± 0.0

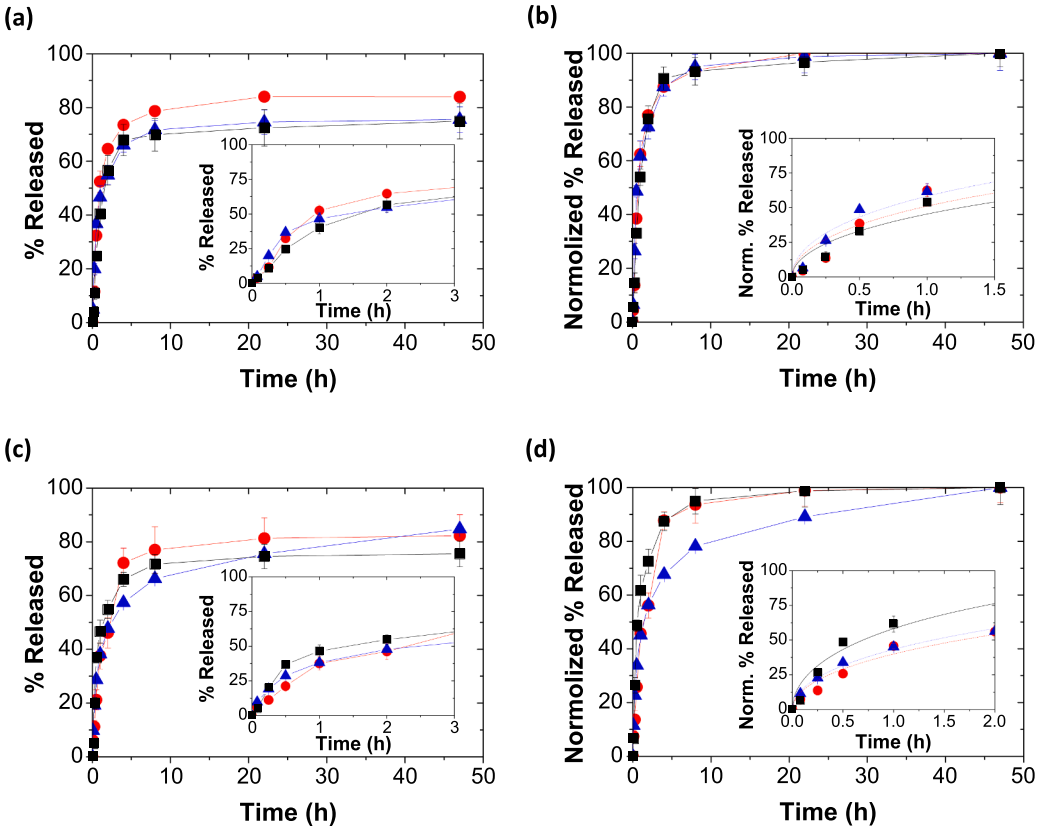

Fig. 6. Actual (a, c) and normalized (b, d) BSA release profiles obtained from chitosan/TPP particle pellets after (a, b) 30 min of centrifugation at (■) 4.8×10^4, (●) 1.1×10^5 and (▲) 3.0×10^5 *g*, and (c, d) after (■) 30, (●) 60 and (▲) 90 min of centrifugation at 3.0×10^5 *g*. The insets in (a, c) show the first 3 h of the original BSA release profiles and the insets in (b, d) show the first 60% of the normalized BSA release and their model fit curves for pellets prepared by centrifugation at each condition using Eq. (8). The lines in the other plots are guides to the eye. All error bars are standard deviations.

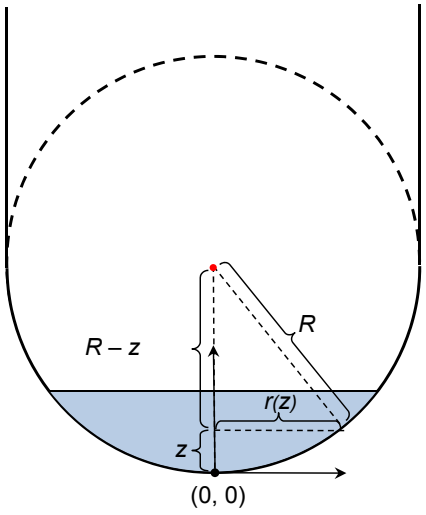

Fig. 7. Schematic of the chitosan/TPP gel pellet formed on the bottom of the centrifuge tube upon ultracentrifugation. The shaded region represents the gel pellet, while the point at the bottom of the tube is the origin of the coordinate system.

the centrifuge tubes (see Table 1). The gel pellet thickness, however, slightly decreased (Table 1). The reduction in the gel pellet thickness (along with the increased chitosan and BSA recovery) again suggested that gel compaction occurred within the pellets. The BSA-loaded chitosan/TPP gel pellets obtained through 30 min of centrifugation resulted in the fastest BSA release (see insets in Fig. 6c and d), which may have reflected their less-compact structure. The BSA release was slower when the centrifugation time increased to 60 and 90 min. Though the release rates varied, the final percentages of BSA released were quite close (ranging between 75 and 84%; see Fig. 6c), regardless of the centrifugation times. Overall, the release profiles obtained from the macroscopic gel pellets were consistent with the apparent release profiles reported in many studies on chitosan/TPP micro- and nanoparticles [59–62], and (when combined with the fact that pellets formed under all centrifugation conditions analyzed in Fig. 3) support the hypothesis that there may have been considerable particle coagulation during centrifugation-assisted release experiments.

3.2.3. Further analysis of release from the chitosan/TPP gel pellets

To better understand the mechanism of protein release from the gel pellets, changes in the pellet mass during the release process were also analyzed. This revealed that the gel mass remained roughly constant (see Supplementary Data, Section E), suggesting that gel swelling and degradation effects were insignificant. Thus, BSA release from the gel pellets was likely diffusion-limited and could be described using a Fickian diffusion equation. For one-dimensional diffusion, the microscopic mass balance needed to determine the time-dependent concentration profile within the gel pellets is given by:

$$\frac{\partial C_A}{\partial t} = \frac{D_A}{A(z)} \frac{\partial}{\partial z}\left(A(z)\frac{\partial C_A}{\partial z}\right) \tag{6}$$

where C_A is the local payload concentration within the gel pellet, t is the release time, D_A is the payload diffusivity within the gel, z is the distance from the bottom of the centrifuge tube and $A(z)$ is the cross-sectional area of the gel pellet at the axial position, z.

Assuming that the inner radius of the centrifuge tube was R (see Fig. 7), the z-dependent radius within the hemispherical bottom of the centrifuge tube could be defined as $r(z)$. Since $A(z)$ equaled to $\pi r^2(z)$ and $r(z) = \sqrt{R^2 - (R-z)^2}$, $A(z)$ could be expressed as $A(z) = \pi(2Rz - z^2)$. Moreover, because the pellet thickness, L, was significantly smaller than R, the z^2 term had a relatively weak contribution (Supplementary Data, Section F) and the "$A(z)$ versus z" scaling was roughly linear. Thus, $A(z)$ was approximated as $2\pi Rz$. Substituting this into Eq. (6) yielded:

$$\frac{\partial C_A}{\partial t} = \frac{D_A}{z}\frac{\partial}{\partial z}\left(z\frac{\partial C_A}{\partial z}\right) \quad (7)$$

This equation had the same functional form as that for the one-dimensional radial release from a cylinder (although here the radical position, r, was replaced with z). Based on a zero-flux boundary condition at $z = 0$ and a perfect-sink boundary condition at $z = L$, Eq. (7) predicts the short-time release to be [63]:

$$\frac{M_t}{M_\infty} = 4\left[\frac{D_A t}{\pi L^2}\right]^{1/2} - \pi\left[\frac{D_A t}{\pi L^2}\right] - \frac{\pi}{3}\left[\frac{D_A t}{\pi L^2}\right]^{3/2} \quad (8)$$

where M_t and M_∞ are the cumulative masses of payload released at time t and infinite time, respectively, D_A is the effective payload diffusivity within the gel matrix, and L is the thickness of the gel pellet at the center of the tube. This solution is valid for the first 60% of the release process [63]. Thus, the apparent diffusivity can be determined by fitting the release profile to Eq. (8) as shown in the insets to Fig. 6b and d.

The apparent protein diffusivities within the gel pellets prepared using different centrifugation conditions (which, despite the imperfect model fits, could be roughly estimated) are summarized in Table 1. As the centrifugal force increased (from 4.8×10^4 to 3.0×10^5 g), the apparent BSA diffusivity did not change much and remained in the 3.4–3.8 $\times 10^7$ cm^2/s range, despite the apparent gel compression (which was evidenced by a reduced gel thickness; see Table 1). As the centrifugation time increased from 30 to 60 min, however, the apparent BSA diffusivity dropped from 3.8×10^{-7} to 1.1×10^{-7} cm^2/s, and remained almost unchanged as the centrifugation time increased further (Table 1). The BSA diffusivities inside the chitosan/TPP gels were on the same order of magnitude as their diffusivity in water (9.3×10^{-7} cm^2/s at 37 °C [64]). This high BSA diffusivity suggested that the mesh size of the gel network remained larger than the BSA molecule, despite the apparent gel compression during centrifugation.

Collectively, the release rates obtained using the chitosan/TPP gel pellets could help understand what might happen during the release experiments on chitosan/TPP micro- and nanoparticles. The apparent diffusion coefficients, which were on the same order as those of BSA in water, indicated the BSA/particle binding to be weak during the release process (otherwise, the apparent diffusivities inside the gels would have been significantly lower [65]). This weak BSA/particle binding might reflect the elevated pH of PBS (pH 7.4), which deprotonated the chitosan and eliminated most of its ionic interaction with BSA [36]. The high BSA diffusivities measured herein were also on the same order as those reported in other (anionic and nonionic) polysaccharide hydrogels at 37 °C (such as 1–2 wt% covalently crosslinked hyaluronan and 3 wt% agarose, where $D_A \approx$ 3–5 $\times 10^{-7}$ cm^2/s [66,67]), which further supported the above interpretation of the high BSA diffusivities within the chitosan/TPP gel pellets.

The water content of the most extensively centrifuged chitosan/TPP gel pellets was estimated at about 93 wt% (based on their weight loss upon drying in a 60 °C oven), confirming that the chitosan/TPP networks are water-rich [30,68]. Additionally, compared to the compressed gel pellets formed upon ultracentrifugation, dispersed chitosan/TPP micro- and nanoparticles (which do not undergo centrifugation-induced compression) might have a sparser gel network structure. Therefore, BSA diffusivity within the particles is likely no less than that in the gel pellet. Due to their high surface-to-volume ratio, however, the micro- and nanoparticles may be less stable to dissociation when placed in PBS [42]. This reduced stability, and their much lower diffusion path length, should make BSA release from the chitosan/TPP micro- and nanoparticles much faster than that from the macroscopic chitosan/TPP gel pellets. Indeed, even when the gel pellets are cut into smaller pieces (approximately 0.1–1 mm in size) BSA release becomes much faster and more complete (see Supplementary Data, Section G).

A number of reports (including the widely cited BSA release study by Gan and Wang [59]) have shown BSA release into 37 °C PBS from chitosan/TPP particles to occur over several hours before reaching a plateau [59,60,69]. These reports, however, did not indicate the use of any techniques (such as using a glycerol bed) for redispersing particles after centrifugation. Because coagulated chitosan/TPP particles are very difficult to redisperse to their original micro- and nanoscale state (even after the ultrasonic treatment or vigorous agitation), it is possible that these multiple-hour release times resulted from irreversible particle coagulation. Thus, it is essential to prevent irreversible coagulation during the centrifugation step. To our knowledge, the only method that has (occasionally) been utilized to achieve this was the use of a glycerol bed [11,27,28]. This approach was also utilized to prevent chitosan/TPP particle coagulation here, when studying release from micro- and nanoparticle dispersions, and its efficacy will be discussed further in Section 3.3.3.

3.3. Release from dispersed particles: Ionic strength and sampling frequently effects

3.3.1. Ionic strength effects

To test the hypothesis (advanced in the Introduction) that the multiple-day release reported in the seminal studies on chitosan/TPP nanoparticles may have been an artifact of using salt-free release media, the effect of ionic strength was first explored; specifically, by comparing the BSA release profiles obtained in 5 wt% trehalose solution with either 0 mM NaCl (as used by Calvo et al. [34,35]) or 150 mM NaCl (i.e., near-physiological ionic strength). When the BSA-loaded chitosan/TPP particles were placed in 0 mM NaCl trehalose solution, the release was much slower (Fig. 8). Only about 30% of BSA was released after 1 h and less than 45% of BSA was released after 6 h. In 150 mM NaCl media, however (which was more representative of physiological conditions), more than 90% of the BSA was released from the particles within 1 h.

Since the pH of the release media was similar to the pH where the particles were formed, this near-complete BSA release mainly reflected the increased ionic strength, which caused the dissociation of BSA from the chitosan/TPP micro- and nanoparticles. The rapid release of the dissociated protein may also have reflected the small size of the chitosan/TPP particles. Indeed, most papers that used glycerol beds to redisperse the chitosan/TPP particles, also showed a burst protein release into PBS (fast release at the first time point), whereupon the release curve reached a plateau [11,70–72]. Thus, the sustained multiple-day release obtained from chitosan/TPP nanoparticles in the seminal studies [34,35] was likely caused by the salt-free conditions used in that work.

3.3.2. Sampling frequency effects

Given the rapid protein release from colloidal chitosan/TPP particles predicted from the high D_A-values (see Section 3.2), the apparent release profile could also be affected by the solvent replacement frequency – i.e., equilibrium payload partitioning between the particles and the release media might be reached sooner than the time interval

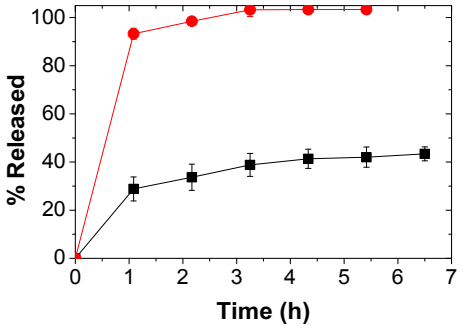

Fig. 8. The ionic strength effect on the BSA release profile in the 5% trehalose solution (pH 6.0) with (■) 0 and (●) 150 mM NaCl. The error bars are standard deviations and the lines are guides to the eye.

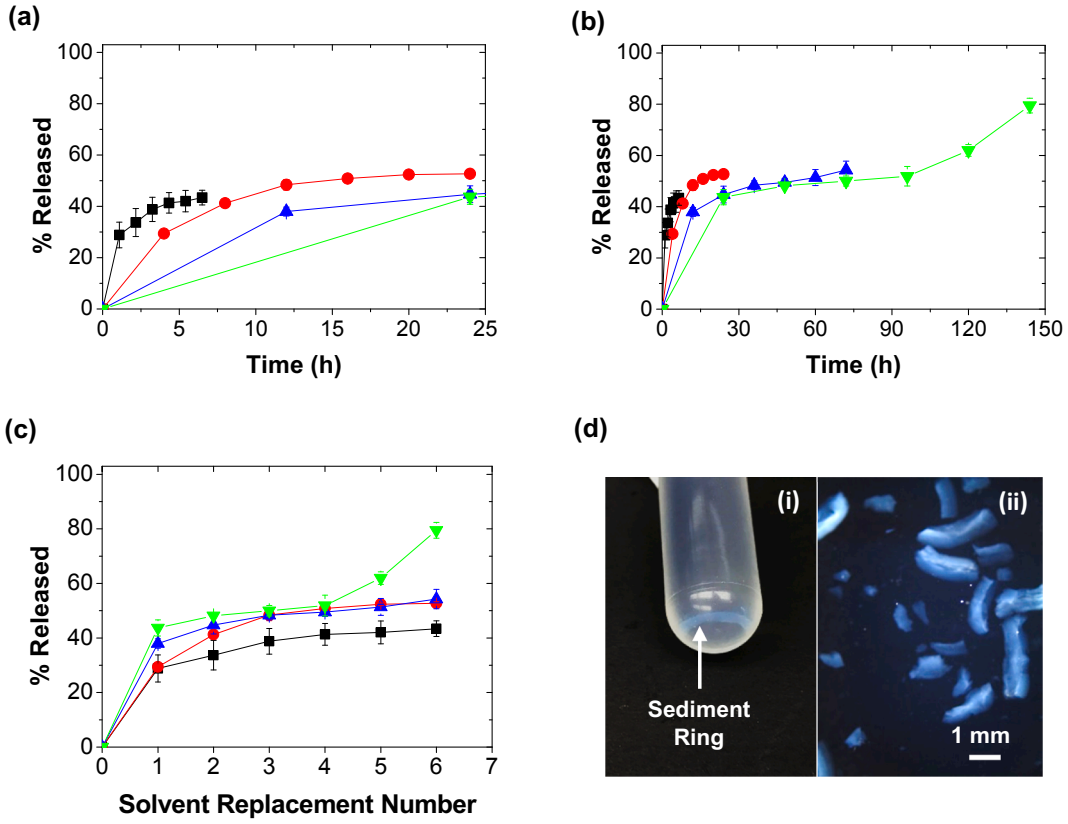

Fig. 9. BSA release into 5 wt% trehalose solution at pH 6.0 and 0 mM NaCl, obtained using (■) 1, (●) 4, (▲) 12 and (▼) 24 h time intervals between the solvent replacement steps, plotted versus the: (a, b) release time, shown here (a) for the first day and (b) the whole experiment, (c) number of solvent replacement steps; and (d) photos showing particle coagulation after three centrifugation cycles with a glycerol bed taken (i) before and (ii) after vortexing. The error bars are standard deviations and the lines are guides to the eye.

between the sampling/solvent replacement steps. To investigate this possibility, Fig. 9a and b compare the release profiles obtained using 1, 4, 12 and 24 h intervals between solvent replacements. The release profile obtained using the 1 h time interval showed faster BSA release compared to that with the 4 h time interval (Fig. 9a). This indicates that sink conditions are not maintained with the 4 h interval time and that accumulation of BSA in the release medium impedes further release. Similar trends emerge when data obtained with the 4 h interval are compared with that with the 12 h interval. Interestingly, however, the release profiles achieved with the 12 and 24 h solvent replacement time intervals were partially overlapped (Fig. 9a and b).

The differences in these release profiles confirmed that the measured BSA release profiles could indeed depend strongly on the solvent replacement frequency. Moreover, when the release profiles were plotted versus the number of solvent replacement steps rather than versus time, the release profiles (which appeared to vary in Fig. 9a and b) became similar to one another (Fig. 9c). Each curve started with a 30–45% burst release at the first sampling point, followed by a much slower BSA release rate. This biphasic release may have stemmed from some protein binding sites being stronger than others (possibly due to nonuniform distributions of protein-associating moieties within the particles), which may have made BSA/chitosan binding to certain particle regions strong enough to slow some of the protein release into the NaCl-free release medium. This view is consistent with recent findings by Sacco et al., who have shown the chitosan/TPP matrix to (at least at the macroscopic scale) be inhomogeneous [73].

The release curve with the 1 h time interval was slightly lower than those with longer time intervals (Fig. 9c). This suggests that, though there is significant BSA accumulation in the release medium after 1 h of contact time (which means that sink conditions are not maintained), equilibrium BSA partitioning is (at least in some of the sampling steps) not yet achieved. At higher time intervals, however, the curves in Fig. 9c significantly overlap, indicating that equilibrium partitioning is, for the most part, nearly reached and that the apparent release profiles obtained using the solvent replacement method (Fig. 9a and b) are artifacts of the solvent replacement frequency used.

Interestingly, after the fourth solvent replacement, for the release profile obtained using a 24 h solvent replacement interval time, the percent released became higher than that with shorter time intervals (Fig. 9c). This may have been caused by TPP and/or chitosan degradation [74–76], which may have led to partial particle dissociation during the longer, 6-day duration of the release experiments with the 24 h interval time between the solvent replacement steps. Overall, the above findings indicate that, to avoid non-sink conditions and/or "equilibrium partitioning artifacts," a more frequent solvent replacement is preferred if the release is fast (which appears to be the case for chitosan/TPP micro- and nanoparticles). Conversely, if the release is slow, a less frequent solvent replacement is desired to minimize the "extra release" caused by the incomplete recovery of micro- and nanoparticles during centrifugation (see Fig. 4).

Besides analyzing the differences in release profiles obtained in this study, it is instructive to compare our results with those in the seminal studies by Calvo *et al.* [34,35]. Compared to the BSA release profiles in Fig. 9 (obtained using 1–24 h solvent replacement intervals), Calvo et al. (who used a 2-day solvent replacement interval) reported a much slower release rate with release times that exceeded 1 week [34,35]. Plotting the BSA release profile versus the solvent replacement number, however, showed the data reported by Calvo et al. to be quite similar to ours (see Fig. 10). In both cases, 25–45% of the BSA was released by the first solvent replacement step and about 50% of the BSA was released after the fourth solvent replacement in both studies (with the moderate quantitative differences between the two data sets possibly reflecting

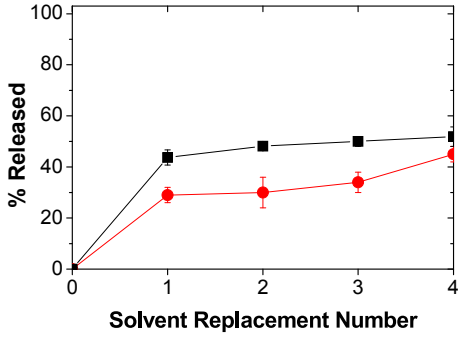

Fig. 10. BSA release into 5% trehalose solution obtained (■) in this work using the 24 h time interval between the solvent replacement steps and (●) in Calvo's work using a 2-day time interval between the solvent replacement steps. The error bars are standard deviation and the lines are guides to the eye.

compositional differences between the particles used in the two studies). This result could imply that the BSA release profile reported by Calvo et al. did not truly reflect its release behavior, since the solvent replacement interval time (2 days) substantially exceeded the time needed to reach equilibrium BSA partitioning between the particles and the receiving media. The same might apply to other literature release experiments with low sampling frequencies [6,14,15].

3.3.3. Glycerol bed efficiency

As the final part of our analysis of the sample and separate method of characterizing release from submicron chitosan/TPP particles, we turn our attention to the efficacy of the glycerol bed. The glycerol bed, which was used to obtain the release data in Figs. 9 and 10, helps prevent particle coagulation during centrifugation. After 3 or 4 centrifugation/redispersion cycles, however (at least with the 1 h centrifugation steps at $3.0 \times 10^5 g$ needed to achieve near complete particle separation), ring-shaped deposits form on the centrifuge tubes and these coagulated particles cannot be fully redispersed even by extensive vortexing or sonication (Fig. 9d). This coagulation becomes more prevalent with further centrifugation/redispersion cycles, and may slow down release by increasing the diffusion distance for the releasing molecules. Thus, at the centrifugation intensity needed to fully recover the particles, particle coagulation upon centrifugation appears to be challenging to prevent even with a glycerol bed. To avoid this coagulation problem in the release experiment, it may therefore be preferable to, instead of separating the particles by centrifuging the whole dispersion, place the particle dispersions in large volumes of release media (to create true sink conditions) and collect small fractions of these dispersions for testing during sampling times. These small sample fractions can then be sacrificed for analysis – i.e., by separating the particles from the supernatant (through either centrifugation or filtration) and analyzing the supernatant for the released solute content. Here, filtration might also accelerate particle separation from the supernatant [25] and, to help maintain sink conditions in rapidly releasing dispersions, could drastically reduce the time increments between solvent replacement steps.

3.4. Other pitfalls

Herein, we analyzed some key pitfalls that can occur when measuring release from chitosan/TPP micro- and nanoparticles. Yet, there are several other cautionary points that are worth making. The first is that it is important to measure and report the chitosan/TPP particle amounts used during the release experiments. This is because dispersion concentrations can affect payload molecule/particle association, chitosan/TPP association and, due to the chitosan and TPP buffering capacity, the release media pH [42]. Thus, particle concentrations can affect both the release profiles and, as shown by us recently [42], particle stabilities. This vital information on how much chitosan, TPP and releasing payload is initially added to the release media, however, is often missing from literature on chitosan/TPP micro- and nanocarriers.

Another potential pitfall (that is not addressed above) arises from artifacts in released molecule quantification, especially where simple UV–vis spectroscopy is used, where light scattering from the release media at low (ultraviolet) wavelengths can be misinterpreted as absorbance from the released molecules [77]. Scattering from debris in the release media can, therefore, if care is not taken, be misinterpreted to overestimate the release rates (or to even show release where none occurs). Finally, because chitosan/TPP and chitosan/payload molecule interactions can depend on chitosan DD and molecular weight [42,54], some variability in the reported release performance may reflect differences in the chitosans used. It is therefore essential to report both the chitosan molecular weights/DD-values and particle (and release media) quantities used in all release studies. Collectively, these considerations (along with the artifacts analyzed in this study) show that release experiments on chitosan/TPP nanoparticles and other ionically crosslinked colloids must be undertaken with utmost caution and add to the growing literature on the limitations of conventional release experiments [25,26,39–41].

4. Conclusions

We have shown that the apparent release profiles measured from chitosan/TPP micro- and nanoparticles using the common, centrifugation-assisted "sample and separate" method can be affected by: (1) incomplete particle separation from the release media; (2) particle size change due to their centrifugation-induced coagulation; and (3) sink conditions not being achieved due to an insufficient solvent replacement frequency. To minimize problems with incomplete particle separation, high centrifugal forces and long centrifugation times (which exceed those used typically) are needed. A glycerol bed can help prevent particle coagulation; however, this method no longer appears to work for chitosan/TPP micro- and nanoparticles after the first 3–4 centrifugation/redispersion cycles (at least under the centrifugation conditions needed for their full separation with our setup). For particles with fast release rates (such as the colloidal chitosan/TPP particles explored in this work), frequent sampling/solvent replacement must also be used to capture the release kinetics and maintain sink conditions. Due to the long centrifugation times required to fully sediment the particles, however, this ultracentrifugation-assisted solvent replacement method cannot accurately determine the release profiles. As an alternative, sink conditions can likely be achieved by diluting the dispersions in large volumes of release media and collecting small dispersion portions to (after removing the particles with a filter) quantify the release. Besides examining the sample and separate method, we show that it is essential to use release media with physiologically relevant ionic strength levels, as release from chitosan/TPP particles can be highly salt-sensitive. Although this work focused only on chitosan/TPP micro- and nanoparticles, the experimental artifacts highlighted by this study likely extend to other micro- and nanocarrier systems, such as other polyelectrolyte-based particles [78,79], and (as discussed in prior reports [25,26,39–41]) even other polymer colloids, emulsions and liposomes [40,80,81]. Overall, we have demonstrated that procedures for quantifying bioactive payload release from chitosan/TPP micro- and nanoparticles, and related systems must be selected with great care.

Acknowledgement

The authors gratefully acknowledge the National Science Foundation (CBET-1133795) for supporting this work and Prof. Tomer Avidor-Reiss (Univ. of Toledo) for the use of the ultracentrifuge in his lab.

Appendix A. Supplementary material

Supplementary data to this article can be found online at https://doi.org/10.1016/j.ejpb.2019.06.020.

References

[1] M. Garcia-Fuentes, M.J. Alonso, Chitosan-based drug nanocarriers: where do we stand? J. Controlled Release 161 (2012) 496–504.
[2] H. Katas, H.O. Alpar, Development and characterisation of chitosan nanoparticles for siRNA delivery, J. Controlled Release 115 (2006) 216–225.
[3] A. Vila, A. Sánchez, K. Janes, I. Behrens, T. Kissel, J.L. VIla-Jato, M.J. Alonso, Low molecular weight chitosan nanoparticles as new carriers for nasal vaccine delivery in mice, Eur. J. Pharm. Biopharm. 57 (1) (2004) 123–131.
[4] S. Vimal, S.A. Majeed, K. Nambi, N. Madan, M. Farook, C. Venkatesan, G. Taju, S. Venu, R. Subburaj, A. Thirunavukkarasu, Delivery of DNA vaccine using chitosan–tripolyphosphate (CS/TPP) nanoparticles in Asian sea bass, Lates calcarifer (Bloch, 1790) for protection against nodavirus infection, Aquaculture 420 (2014) 240–246.
[5] C. Colonna, B. Conti, P. Perugini, F. Pavanetto, T. Modena, Chitosan glutamate nanoparticles for protein delivery: development and effect on prolidase stability, J. Microencapsulation 24 (2007) 553–564.
[6] Y. Hou, J. Hu, H. Park, M. Lee, Chitosan-based nanoparticles as a sustained protein release carrier for tissue engineering applications, J. Biomed. Mater. Res. A 100 (2012) 939–947.
[7] I.A. Sogias, A.C. Williams, V.V. Khutoryanskiy, Why is chitosan mucoadhesive? Biomacromolecules 9 (2008) 1837–1842.
[8] D. Vllasaliu, R. Exposito-Harris, A. Heras, L. Casettari, M. Garnett, L. Illum, S. Stolnik, Tight junction modulation by chitosan nanoparticles: comparison with chitosan solution, Int. J. Pharm. 400 (2010) 183–193.
[9] X. Wang, N. Chi, X. Tang, Preparation of estradiol chitosan nanoparticles for improving nasal absorption and brain targeting, Eur. J. Pharm. Biopharm. 70 (2008) 735–740.
[10] R. Fernández-Urrusuno, P. Calvo, C. Remuñán-López, J.L. Vila-Jato, M.J. Alonso, Enhancement of nasal absorption of insulin using chitosan nanoparticles, Pharm. Res. 16 (10) (1999) 1576–1581.
[11] A. Grenha, B. Seijo, C. Remunán-López, Microencapsulated chitosan nanoparticles for lung protein delivery, Eur. J. Pharm. Sci. 25 (4–5) (2005) 427–437.
[12] K.A. Janes, M.J. Alonso, Depolymerized chitosan nanoparticles for protein delivery: preparation and characterization, J. Appl. Polym. Sci. 88 (2003) 2769–2776.
[13] C. Bulmer, A. Margaritis, A. Xenocostas, Production and characterization of novel chitosan nanoparticles for controlled release of rHu-Erythropoietin, Biochem. Eng. J. 68 (2012) 61–69.
[14] S. Jarudilokkul, A. Tongthammachat, V. Boonamnuayvittaya, Preparation of chitosan nanoparticles for encapsulation and release of protein, Korean J. Chem. Eng. 28 (5) (2011) 1247.
[15] W. Yang, J. Fu, T. Wang, N. He, Chitosan/sodium tripolyphosphate nanoparticles: preparation, characterization and application as drug carrier, J. Biomed. Biotechnol. 5 (5) (2009) 591–595.
[16] Y. Luo, B. Zhang, W.-H. Cheng, Q. Wang, Preparation, characterization and evaluation of selenite-loaded chitosan/TPP nanoparticles with or without zein coating, Carbohydr. Polym. 82 (3) (2010) 942–951.
[17] L. Calderon, R. Harris, M. Cordoba-Diaz, M. Elorza, B. Elorza, J. Lenoir, E. Adriaens, J.P. Remon, A. Heras, D. Cordoba-Diaz, Nano and microparticulate chitosan-based systems for antiviral topical delivery, Eur. J. Pharm. Sci. 48 (2013) 216–222.
[18] M. Kaloti, H.B. Bohidar, Kinetics of coacervation transition versus nanoparticle formation in chitosan-sodium tripolyphosphate solutions, Colloids Surf. B 81 (2010) 165–173.
[19] R.C. Nagarwal, P.N. Singh, S. Kant, P. Maiti, J.K. Pandit, Chitosan nanoparticles of 5-fluorouracil for ophthalmic delivery: characterization, in-vitro and in-vivo study, Chem. Pharm. Bull. 59 (2011) 272–278.
[20] Y. Lapitsky, Ionically crosslinked polyelectrolyte nanocarriers: recent advances and open problems, Curr. Opinion Colloid Interface Sci. 19 (2) (2014) 122–130.
[21] C. Washington, Evaluation of non-sink dialysis methods for the measurement of drug release from colloids: effects of drug partition, Int. J. Pharm. 56 (1) (1989) 71–74.
[22] Y. Zambito, E. Pedreschi, G. Di Colo, Is dialysis a reliable method for studying drug release from nanoparticulate systems?—a case study, Int. J. Pharm. 434 (1–2) (2012) 28–34.
[23] G. Moreno-Bautista, K.C. Tam, Evaluation of dialysis membrane process for quantifying the in vitro drug-release from colloidal drug carriers, Colloids Surf. A 389 (1–3) (2011) 299–303.
[24] Y. Cai, Y. Lapitsky, Analysis of chitosan/tripolyphosphate micro- and nanogel yields is key to understanding their protein uptake performance, J. Colloid Interface Sci. 494 (2017) 242–254.
[25] J. Shen, D.J. Burgess, In vitro dissolution testing strategies for nanoparticulate drug delivery systems: recent developments and challenges, Drug Deliv. Transl. Res. 3 (5) (2013) 409–415.
[26] S.J. Wallace, J. Li, R.L. Nation, B.J. Boyd, Drug release from nanomedicines: selection of appropriate encapsulation and release methodology, Drug Deliv. Transl. Res. 2 (4) (2012) 284–292.
[27] E. Bahreini, K. Aghaiypour, R. Abbasalipourkabir, A.R. Mokarram, M.T. Goodarzi, M. Saidijam, Preparation and nanoencapsulation of L-asparaginase II in chitosan-tripolyphosphate nanoparticles and in vitro release study, Nanoscale Res. Lett. 9 (1) (2014) 340.
[28] N. Csaba, M. Koping-Hoggard, M.J. Alonso, Ionically crosslinked chitosan/tripolyphosphate nanoparticles for oligonucleotide and plasmid DNA delivery, Int. J. Pharm. 382 (2009) 205–214.
[29] Q. Gan, T. Wang, C. Cochrane, P. McCarron, Modulation of surface charge, particle size and morphological properties of chitosan-TPP nanoparticles intended for gene delivery, Colloids Surf. B 44 (2005) 65–73.
[30] H. Jonassen, A.L. Kjoniksen, M. Hiorth, Effects of ionic strength on the size and compactness of chitosan nanoparticles, Colloid Polym. Sci. 290 (2012) 919–929.
[31] T. Lopez-Leon, E.L.S. Carvalho, B. Seijo, J.L. Ortega-Vinuesa, D. Bastos-Gonzalez, Physicochemical characterization of chitosan nanoparticles: electrokinetic and stability behavior, J. Colloid Interface Sci. 283 (2005) 344–351.
[32] Z. Ma, H.H. Yeoh, L.Y. Lim, Formulation pH modulates the interaction of insulin with chitosan nanoparticles, J. Pharm. Sci. 91 (6) (2002) 1396–1404.
[33] B.P. Koppolu, S.G. Smith, S. Ravindranathan, S. Jayanthi, T.K.S. Kumar, D.A. Zaharoff, Controlling chitosan-based encapsulation for protein and vaccine delivery, Biomaterials 35 (14) (2014) 4382–4389.
[34] P. Calvo, C. Remunan-Lopez, J.L. Vila-Jato, M.J. Alonso, Chitosan and chitosan/ethylene oxide-propylene oxide block copolymer nanoparticles as novel carriers for proteins and vaccines, Pharm. Res. 14 (1997) 1431–1436.
[35] P. Calvo, C. Remunan-Lopez, J.L. Vila-Jato, M.J. Alonso, Novel hydrophilic chitosan-polyethylene oxide nanoparticles as protein carriers, J. Appl. Polym. Sci. 63 (1997) 125–132.
[36] A.B. Kayitmazer, S.P. Strand, C. Tribet, W. Jaeger, P.L. Dubin, Effect of polyelectrolyte structure on protein – polyelectrolyte coacervates: coacervates of bovine serum albumin with poly(diallyldimethylammonium chloride) versus chitosan, Biomacromolecules 8 (11) (2007) 3568–3577.
[37] E. Kizilay, A.B. Kayitmazer, P.L. Dubin, Complexation and coacervation of polyelectrolytes with oppositely charged colloids, Adv. Colloid Interface Sci. 167 (1–2) (2011) 24–37.
[38] K.W. Mattison, P.L. Dubin, I.J. Brittain, Complex formation between bovine serum albumin and strong polyelectrolytes: effect of polymer charge density, J. Phys. Chem. B 102 (19) (1998) 3830–3836.
[39] S.S. D'Souza, P.P. DeLuca, Methods to assess in vitro drug release from injectable polymeric particulate systems, Pharm. Res. 23 (3) (2006) 460–474.
[40] A. Bernkop-Schnürch, A. Jalil, Do drug release studies from SEDDS make any sense? J. Control. Release 271 (2018) 55–59.
[41] C. Washington, Drug release from microdisperse systems: a critical review, Int. J. Pharm. 58 (1) (1990) 1–12.
[42] Y. Huang, Y. Cai, Y. Lapitsky, Factors affecting the stability of chitosan/tripolyphosphate micro- and nanogels: resolving the opposing findings, J. Mater. Chem. B 3 (2015) 5957–5970.
[43] Y. Lapitsky, T. Zahir, M.S. Shoichet, Modular biodegradable biomaterials from surfactant and polyelectrolyte mixtures, Biomacromolecules 9 (2008) 166–174.
[44] Glycerine Producers' Association, Physical Properties of Glycerine and Its Solutions, Glycerine Producers Association, New York, 1963.
[45] K.E. Van Holde, W.C. Johnson, P.S. Ho, Principles of Physical Biochemistry, Prentice Hall, Upper Saddle River, 2006.
[46] W.M. Deen, Analysis of Transport Phenomena, Oxford University Press, New York, 1998.
[47] J. Dam, P. Schuck, Calculating sedimentation coefficient distributions by direct modeling of sedimentation velocity concentration profiles, in: M.L. Johnson, L. Brand (Eds.), Methods Enzymol, Elsevier Academic Press, San Diego, 2004, pp. 185–212.
[48] M.A. Lauffer, The size and shape of tobacco mosaic virus particles, J. Am. Chem. Soc. 66 (7) (1944) 1188–1194.
[49] P. Schuck, Size-distribution analysis of macromolecules by sedimentation velocity ultracentrifugation and lamm equation modeling, Biophys. J. 78 (3) (2000) 1606–1619.
[50] L. Korson, W. Drost-Hansen, F.J. Millero, Viscosity of water at various temperatures, J. Phys. Chem. 73 (1) (1969) 34–39.
[51] Z. Liu, Y. Jiao, F. Liu, Z. Zhang, Heparin/chitosan nanoparticle carriers prepared by polyelectrolyte complexation, J. Biomed. Mater. Res. A 83 (3) (2007) 806–812.
[52] A.j. Wan, Y. Sun, W.t. Li, H.l. Li, Transmission electron microscopy and electron diffraction study of BSA-loaded quaternized chitosan nanoparticles, J. Biomed. Mater. Res. B 86(1) (2008) 197–207.
[53] Q. Xu, L. Guo, X. Gu, B. Zhang, X. Hu, J. Zhang, J. Chen, Y. Wang, C. Chen, B. Gao, Y. Kuang, S. Wang, Prevention of colorectal cancer liver metastasis by exploiting liver immunity via chitosan-TPP/nanoparticles formulated with IL-12, Biomaterials 33 (15) (2012) 3909–3918.
[54] Y.M. Xu, Y.M. Du, Effect of molecular structure of chitosan on protein delivery properties of chitosan nanoparticles Int, J. Pharm. 250 (2003) 215–226.
[55] H. Zhang, M. Oh, C. Allen, E. Kumacheva, Monodisperse chitosan nanoparticles for mucosal drug delivery, Biomacromolecules 5 (2004) 2461–2468.
[56] A.L. Zydney, Protein separations using membrane filtration: new opportunities for whey fractionation, Int. Dairy J. 8 (1998) 243–250.
[57] L.M. Weber, C.G. Lopez, K.S. Anseth, Effects of PEG hydrogel crosslinking density on protein diffusion and encapsulated islet survival and function, J. Biomed. Mater. Res. A 90 (3) (2009) 720–729.
[58] D.Y. Arifin, L.Y. Lee, C.-H. Wang, Mathematical modeling and simulation of drug release from microspheres: implications to drug delivery systems, Adv. Drug Del. Rev. 58 (12–13) (2006) 1274–1325.
[59] Q. Gan, T. Wang, Chitosan nanoparticle as protein delivery carrier-systematic examination of fabrication conditions for efficient loading in release, Colloids Surf. B 59 (2007) 24–34.
[60] C. Mattu, R. Li, G. Ciardelli, Chitosan nanoparticles as therapeutic protein

nanocarriers: the effect of pH on particle formation and encapsulation efficiency, Polym. Compos. 34 (9) (2013) 1538–1545.
[61] Y. Sun, A. Wan, Preparation of nanoparticles composed of chitosan and its derivatives as delivery systems for macromolecules, J. Appl. Polym. Sci. 105 (2) (2007) 552–561.
[62] H.-L. Zhang, S.-H. Wu, Y. Tao, L.-Q. Zang, Z.-Q. Su, Preparation and characterization of water-soluble chitosan nanoparticles as protein delivery system, J. Nanomater. 2010 (2010) 898910.
[63] P.L. Ritger, N.A. Peppas, A simple equation for description of solute release I. Fickian and non-fickian release from non-swellable devices in the form of slabs, spheres, cylinders or discs, J. Control. Release 5 (1) (1987) 23–36.
[64] A. Fardet, C. Hoebler, G. Djelveh, J.-L. Barry, Restricted bovine serum albumin diffusion through the protein network of pasta, J. Agric. Food Chem. 46 (11) (1998) 4635–4641.
[65] M. Singh, J.A. Lumpkin, J. Rosenblatt, Mathematical modeling of drug release from hydrogel matrices via a diffusion coupled with desorption mechanism, J. Control. Release 32 (1) (1994) 17–25.
[66] J.B. Leach, C.E. Schmidt, Characterization of protein release from photocrosslinkable hyluronic acid-polyethylene glycol hydrogel tissue engineering scaffolds, Biomaterials 26 (2005) 125–135.
[67] S. Liang, J. Xu, L. Weng, H. Dai, X. Zhang, L. Zhang, Protein diffusion in agarose hydrogel in situ measured by improved refractive index method, J. Control. Release 115 (2) (2006) 189–196.
[68] J. Li, Q. Huang, Rheological properties of chitosan-tripolyphosphate complexes: from suspensions to microgels Carbohydr, Polym. 87 (2012) 1670–1677.
[69] B. Hu, C.L. Pan, Y. Sun, Z.Y. Hou, H. Ye, X.X. Zeng, Optimization of fabrication parameters to produce chitosan-tripolyphosphate nanoparticles for delivery of tea catechins, J. Agric. Food Chem. 56 (2008) 7451–7458.
[70] M. Alonso-Sande, M. Cuna, C. Remunan-Lopez, D. Teijeiro-Osorio, J.L. Alonso-Lebrero, M.J. Alonso, Formation of new glucomannan − chitosan nanoparticles and study of their ability to associate and deliver proteins, Macromolecules 39 (12) (2006) 4152–4158.
[71] A. Grenha, C. Remuñán-López, E.L.S. Carvalho, B. Seijo, Microspheres containing lipid/chitosan nanoparticles complexes for pulmonary delivery of therapeutic proteins, Eur. J. Pharm. Biopharm. 69 (2008) 83–93.
[72] A.H. Krauland, M.J. Alonso, Chitosan/cyclodextrin nanoparticles as macromolecular drug delivery system, Int. J. Pharm. 340 (1–2) (2007) 134–142.
[73] P. Sacco, F. Brun, I. Donati, D. Porrelli, S. Paoletti, G. Turco, On the correlation between the microscopic structure and properties of phosphate-cross-linked chitosan gels, ACS Appl. Mater. Interfaces 10 (13) (2018) 10761–10770.
[74] C. Chang, G. Racz, Effects of temperature and phosphate concentration on rate of sodium pyrophosphate and sodium tripolyphosphate hydrolysis in soil, Can. J. Soil Sci. 57 (3) (1977) 271–278.
[75] Y.-J. Jeon, F. Shahidi, S.-K. Kim, Preparation of chitin and chitosan oligomers and their applications in physiological functional foods, Food Rev. Int. 16(2) (2000) 159-176.
[76] K. Vårum, M. Ottøy, O. Smidsrød, Acid hydrolysis of chitosans, Carbohydr. Polym. 46 (1) (2001) 89–98.
[77] W. Mäntele, E. Deniz, UV–VIS absorption spectroscopy: Lambert-Beer reloaded, Spectrochim. Acta A 173 (2017) 965–968.
[78] F.M. Goycoolea, G. Lollo, C. Remunan-Lopez, F. Quaglia, M.J. Alonso, Chitosan-alginate bended nanoparticles as carriers for the transmucosal delivery of macromolecules, Biomacromolecules 10 (7) (2009) 1736–1743.
[79] J.-O. You, C.-A. Peng, Calcium-alginate nanoparticles formed by reverse microemulsion as gene carriers, Macromol. Symp. 219 (1) (2005) 147–153.
[80] N.O. Dhoot, M.A. Wheatley, Microencapsulated liposomes in controlled drug delivery: strategies to modulate drug release and eliminate the burst effect, J. Pharm. Sci. 92 (3) (2003) 679–689.
[81] Z. Zhang, S.-S. Feng, The drug encapsulation efficiency, in vitro drug release, cellular uptake and cytotoxicity of paclitaxel-loaded poly (lactide)–tocopheryl polyethylene glycol succinate nanoparticles, Biomaterials 27 (21) (2006) 4025–4033.